Double Linker Triphenylamine Dyes for Dye-Sensitized Solar Cells

Peter J. Holliman[1,*], Moneer Mohsen [2], Arthur Connell [1], Christopher P. Kershaw [1], Diana Meza-Rojas [1], Eurig W. Jones [1], Dawn Geatches [3], Kakali Sen [3] and Ya-Wen Hsiao [3]

[1] College of Engineering, Bay Campus, Swansea University, Swansea SA1 8EN, UK; arthur.connell@swansea.ac.uk (A.C.); c.p.kershaw@swansea.ac.uk (C.P.K.); D.E.Mezarojas@Swansea.ac.uk (D.M.-R.); Eurig.W.Jones@Swansea.ac.uk (E.W.J.)

[2] Ministry of Science and Technology, Materials Research Directorate, Baghdad, Iraq; moneer.69nm@yahoo.com (M.M.)

[3] Scientific Computing Department, STFC Daresbury Laboratory, Daresbury, Warrington WA4 4AD, UK; dawn.geatches@stfc.ac.uk (D.G.); kakali.sen@stfc.ac.uk (K.S.); ya-wen.hsiao@stfc.ac.uk (Y.-W.H.)

* Correspondence: p.j.holliman@swansea.ac.uk

Received: 31 July 2020; Accepted: 03 September 2020; Published: 07 September 2020

Abstract: Most organic dyes synthesized for dye-sensitized solar cells (DSC) use a single linker group to bind to the metal oxide photo-anode. Here we describe the synthesis and testing of two new triphenylamine dyes containing either two carboxylic acids 5-[2-(4-diphenylamino-phenyl)-vinyl]-isophthalic acid (**10**) or two cyanoacrylic acids (2Z, 2′Z)−3, 3′-(5-((E)-4-(diphenylamino) styryl)-1, 3-phenylene) bis (2-cyanoacrylic acid) (**8**) as linker groups. Full characterization data are reported for these dyes and their synthetic intermediates. DSC devices have been prepared from these new dyes either by passive or fast dyeing and the dyes have also been tested in co-sensitized DSC devices leading to a PCE (η = 5.4 %) for the double cyanoacrylate linker dye (**8**) co-sensitized with D149. The dye:TiO_2 surface interactions and dye excitations are interpreted using three modelling methods: density functional theory (at 0 K); molecular dynamics (at 298 K); time dependent density functional theory. The modelling results show the preferred orientation of both dyes on an anatase (1 0 1) TiO_2 surface to be horizontal, and both the simulated and experimental absorption spectra of the dye molecules indicate a red shifted band for (**8**) compared to (**10**). This is in line with broader light harvesting and J_{sc} for (**8**) compared to (**10**).

Keywords: light harvesting; co-sensitization; surface engineering; synthesis; solar energy; atomistic modelling; DFT; MD; TDDFT

ELECTRONIC SUPPLEMENTARY MATERIALS

Synthesis of diphenyl-(4-vinyl-phenyl)-amine (1).

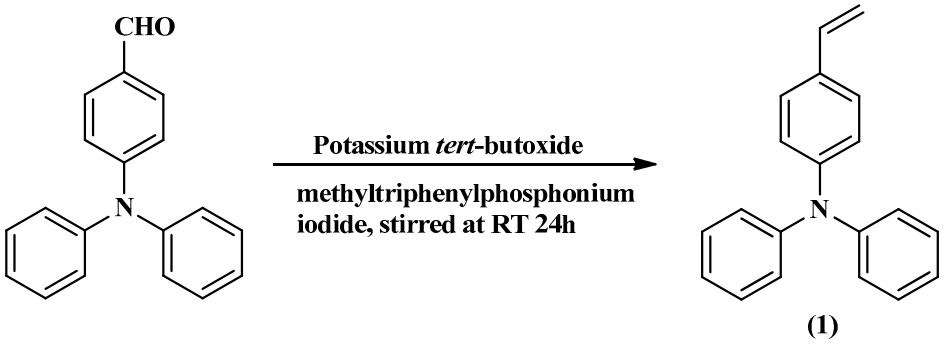

Scheme S1 Synthetic pathway of diphenyl-(4-vinyl-phenyl)-amine (1).

4-(N, N-diphenylamino)-benzaldehyde (7.5 g, 27.46 mmol) was dissolved in (20 ml) of distilled THF under N_2 and added to a mixture of potassium *tert*-butoxide (4.62 g, 41.19 mmol) and methyl triphenyl phosphonium iodide (16.65 g, 41.19 mmol). This reaction mixture was stirred at room temperature for 24 h under nitrogen. The solution was then poured into a mixture of distilled water / methylene chloride (1:1, v/v) and the organic layer separated in a separating funnel, dried over anhydrous magnesium sulfate and the solvent removed in *vacuo*. The product was purified by column chromatography on silica gel in n-hexane/ methylene chloride (95:5, v/v) as eluent. The pure product was identified by TLC and precipitated in methylene chloride/methanol (1:20, v/v) to give diphenyl-(4-vinyl-phenyl)-amine (**1**) as a white solid (yield 5.40 g, 72.5%), m.p. 92–93 °C.

FTMS$^+$-MS: Accurate Mass), reference compound: NH_4OAc, calcd. for $C_{20}H_{17}N$ 272.1437; found 272.1434 $[M+H]^+$. ^1H NMR (500 MHz, DMSO-d6) δ 5.15 (d, J = 11.0 Hz, 1H, H-*CH*=CH-), 5.68 (d, J = 17.6 Hz, 1H, *H*-CH=CH-), 6.66 (dd, J = 10.7, 17.5 Hz, 1H, CH_2=*CH*-), 6.92 (d, J = 8.5 Hz, 2H, =CH-*Ph*-N-), 7.00 (d, J = 8.5 Hz, 4H, -N-*Ph*$_2$), 7.04 (t, J = 7.55 Hz, 2H, -N-*Ph*$_2$-), 7.29 (t, J = 7.8 Hz, 4H, -N-*Ph*$_2$), 7.37 (d, J = 8.2 Hz, 2H, =CH-*Ph*-N-). ^{13}C NMR (125 MHz, DMSO-d6) δ 112.46 (-CH=<u>*CH*$_2$-</u>), 123.03, 123.20, 124.03, 127.27, 129.57 (Ar-<u>*C-H*</u>), 131.50 (Ar-<u>*C-C*</u>), 136.02 (Ar-<u>*CH*</u>=CH_2), 146.95, 147.0(Ar-<u>*C-N*</u>). UV-Vis in ethanol: λ_{max} 324 nm. FT-IR spectrum (KBr ν/cm^{-1}): 3084, 3060 and 3032 cm^{-1} ν (C-H, m) aromatic; 2999, 2853 cm^{-1} ν (C-H, m) aliphatic; 1590, 1486 cm^{-1} ν (C=C, s) and 1175 cm^{-1} for ν (C-N, s).

Mass spectrometry$[M+H]^+$ 272.1434, which corresponds to diphenyl-(4-vinyl-phenyl)-amine (**1**), $[M+H]^+$.

Synthesis of 5-bromo−1, 3-di-benzaldehyde (5)

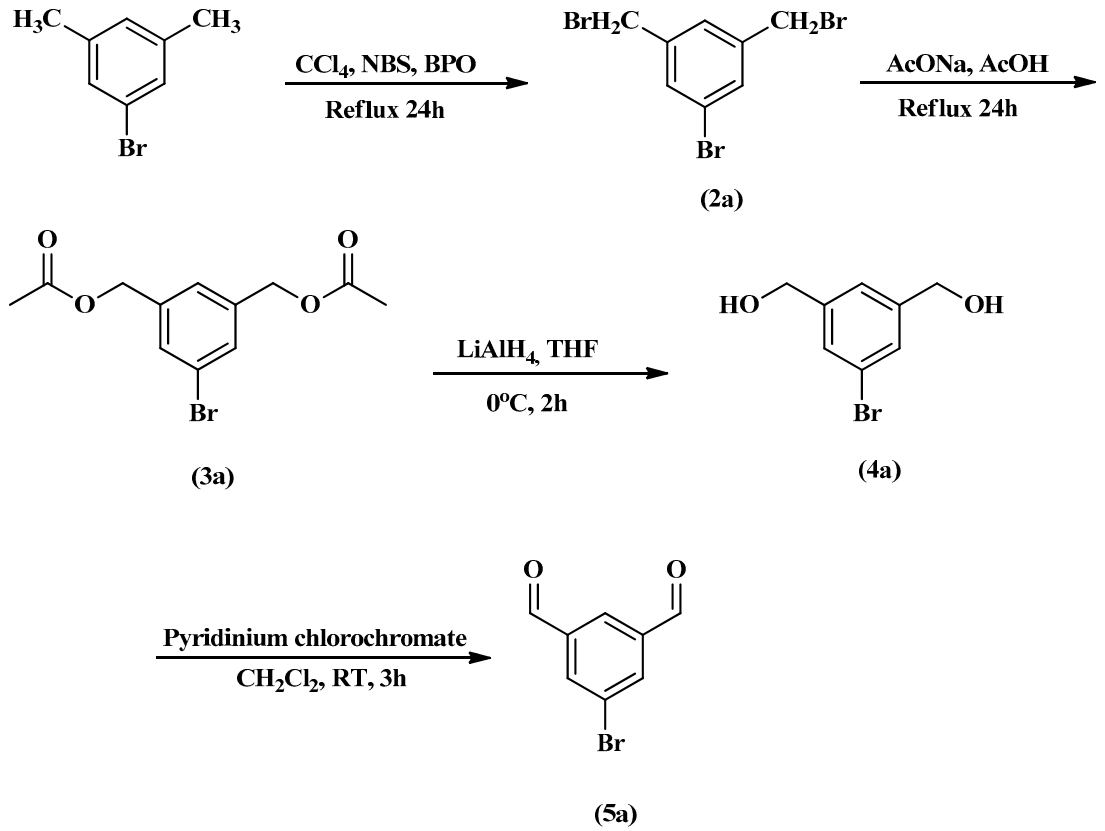

Scheme S2 Synthetic pathway of 5-bromo-1, 3-di-benzaldehyde (5).

Synthesis of 1-bromo-3, 5-bis (bromomethyl) benzene (2)

(2.78 g, 15 mmol) of 5-bromo-m-xylene and N-bromosuccinimide (NBS) (6.6 g, 37 mmol) were added to 150 ml CCl_4 and refluxed under nitrogen overnight in presence of benzoyl peroxide (BPO) (0.3 g). After refluxing the solution was treated with a mixture of petrol\ethylacetate (5:1, v\v), and then refluxed for 30 min, After cooling to room temperature and filtration to remove the solvent, the

crude product was purified by column chromatography on silica gel by using petrol/ethyl acetate (5:2, v/v) as an eluent to produce white precipitate of **(2)** (yield 1.6g, 39%), m.p. 64–66 ^{o}C. A suitable crystal for X-ray analysis was prepared by dissolving this compound in mixture of (dichloromethane/diethyl ether).

FTMS^{+}-MS: m/z (Accurate Mass), reference compound: NH_4OAc, calcd. for $C_8H_7Br_3$ 357.8436, found 357.8437 $[M+NH_4]^{+}$. ^{1}H NMR (500 MHz, $CDCl_3$) δ 4.41 (s, 4H, 2x -*CH*$_2$-Br), 7.34 (bs, 1H, *Ar-H*), 7.48 (d, *J* = 1.55, 2H, *Ar-H*); ^{13}C NMR (125 MHz, $CDCl_3$) δ 31.04 (Ar-*CH*$_2$-Br), 122.71 (Ar-*C-Br*), 128.26, 133.30 (*Ar-C*-H), 140.30 (*Ar-C*-CH_2-).

Synthesis of 5-bromo-1, 3-phenylene-bis (methylene) diacetate (3)

(5 g) of sodium acetate in (100 ml) of glacial acetic acid was added to a solution of (2 g, 0.0058 mmol) of compound (**2**), which was then refluxed overnight. After cooling at room temperature, the solution was poured into a mixture of a saturated solution of sodium bicarbonate/dichloromethane, the aqueous and organic layers were separated by funnel separation and treated the organic layer with anhydrous $MgSO_4$. The solvent was reduced under vacuum and the product extracted by column chromatography on silica gel by using petroleum spirit: ethyl acetate (5:2, v/v) as an eluent to produce compound (**3a**) as a white solid (yield 1.3 g, 76%). FTMS^{+}-MS: m/z (Accurate Mass), reference compound: NH_4OAc, calcd for $C_{12}H_{13}BrO_4$ 318.0335 found 318.0342 $[M+NH_4]^{+}$. ^{1}H NMR (500 MHz, $CDCl_3$) δ 2.09 (s, 6H, 2x-CH_2OCO-*CH*$_3$), 5.04 (s, 4H, 2x-*CH*$_2$-OCO-CH_3), 7.22 (s, 1H, *Ar-H*) 7.43 (s, 2H, *Ar-H*). ^{13}C NMR (125 MHz, $CDCl_3$) δ 20.60 (-*CH*$_3$), 64.99 (-*CH*$_2$), 122.52 (*Ar-C*-Br), 126.16, 130.63 (*Ar-C*-H), 138.31 (*Ar-C*-CH_2-), 170.80 (*C=O*).

Synthesis of 5-bromo-1, 3-phenylene dimethanol (4)

(3.8 g, 12.6 mmol) of (**3**) was added slowly (drop wise) to a solution of $LiAlH_4$ (0.95 g, 25.2 mmol) in THF (180 ml) at 0 °C. This solution was stirred 1 h at 0 °C, and then for 2 h at room temperature, before refluxing for 1 h. After cooling to room temperature, a saturated aqueous solution of sodium sulphate was added drop wise at 0 °C. After filtration through celite, the filtrate was taken and the solvent reduced under vacuum, the product was purified by column chromatography on silica gel using petroleum spirit/ethyl acetate (5:2, v\v) to produce (**4**) as a white precipitate (yield 2.4 g, 88 %), m.p. 788–2 ^{o}C. (GCMS) EI+: m/z, calcd for $C_8H_9BrO_2$ 215.98 found 215.9. ^{1}H NMR (500 MHz, DMSO-d_6) δ 4.48 (s, 4H, 2x-*CH*$_2$OH), 5.33 (bs, 2H, -CH_2*OH*), 7.24 (s, 1H, *Ar-H*), 7.35 (s, 2H, *Ar-H*); ^{13}C (125MHz, DMSO-d_6) δ 62.19 (*CH*$_2$-OH), 121.23 (*Ar-C*-Br), 123.32, 127.21 (*Ar-C*-H), 145.23 (*Ar-C*-CH_2OH).

Synthesis of 5-bromoisophthalaldehyde (5)

To a solution of pyridinium chlorochromate (7.39 g, 34.28 mmol) in 350 ml CH_2Cl_2 was added (2.8 g, 12.89 mmol) of **(4)** which had been pre-dissolved in 120 ml CH_2Cl_2. This was added slowly (drop wise) over more than 60 min. After addition, the solution was left stirring at room temperature for 3 h. It was then poured into a mixture of petroleum spirit/ethyl acetate (10:2, v/v) to form a precipitate, which was then filtered. The solvent was reduced under vacuum and the product purified by column chromatography on silica gel with petroleum spirit/ethyl acetate (5:2, v/v). The solvent was reduced under vacuum to produce a white precipitate of **(5)** (yield 1 g, 37%), m.p. 100–104 ^{o}C. A suitable crystal for X-ray analysis was prepared by dissolving this compound in dichloromethane followed by slow evaporation. GCMS calcd. for $C_8H_5BrO_2$ 213.03 found 213.9 M^{+}. ^{1}H NMR (500 MHz, $CDCl_3$) δ 8.28 (d, *J* = 0.95, 2H, *Ar-H*), 8.32 (t, *J* = 1.25 Hz, 1H, *Ar-H*), 10.06 (s, 2H, 2x-*CHO*); ^{13}C (125 MHz, CDCl3) δ 124.42 (*Ar-C*-Br), 129.26, 137.23 (*Ar-C*-H), 138.45 (*Ar-C*-C=O), 189.50 (*C=O*).

Synthesis of 1, 3-dimethyl 5-bromoisophthalate (6)

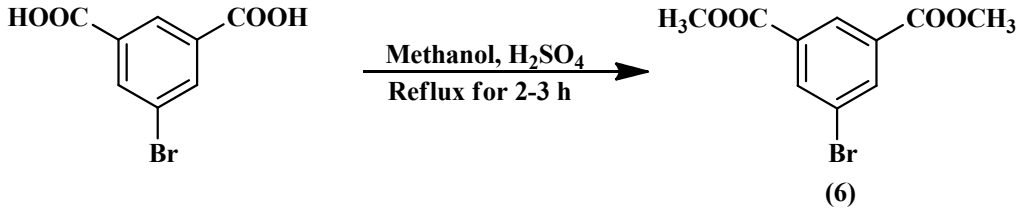

Scheme S3 Synthetic pathway of 1,3-dimethyl 5-bromoisophthalate (6)

5-bromo-isophthalic acid (5 g) was dissolved in 60 ml of methanol, containing 1.4 ml of concentrated H_2SO_4, and this solution was refluxed for 4 h. After cooling at room temperature, 20 ml of a saturated aqueous solution of Na_2CO_3 was added drop wise followed by 100 ml of ethyl acetate. The mixture was separated using a separation funnel. The organic layer was taken and subsequently dried over anhydrous $MgSO_4$. After rotary evaporation of the solvent under reduced pressure, the residue was purified by column chromatography on silica gel with petroleum spirit/ethyl acetate (5:2, v/v). The product was tested using TLC and the product collected after rotary evaporation of the solvent under reduced pressure to produce a white solid of **(6)** (2.0 g, 90 %), m.p. 68–70°C. A suitable crystal for X-ray analysis was prepared by dissolving this compound in dichloromethane followed slow evaporation. FTMS$^+$-MS: m/z (Accurate Mass), reference compound: NH_4OAc, calcd. for $C_{10}H_9BrO_4$ 290.0022, found 290.0028 $[M+NH_4]^+$. ^{1}H NMR (400 MHz, $CDCl_3$) δ 3.97 (s, 6H, 2x-COOC*H*$_3$), 8.36 (d, *J*=1.4, 2H, *Ar-H*), 8.61 (t, *J*=1.4, 1H, *Ar-H*). ^{13}C NMR (100 MHz, $CDCL_3$) δ 52.66 (-<u>*CH*$_3$</u>), 122.57 (<u>*Ar-C*</u>-Br), 129.23, 132.30 (<u>*Ar-C*</u>-H), 136.63 (<u>*Ar-C*</u>-C=O), 164.96 (<u>*C=O*</u>).

Synthesis of (E)-5-(4-(diphenylamino) styryl) isophthalaldehyde (7)

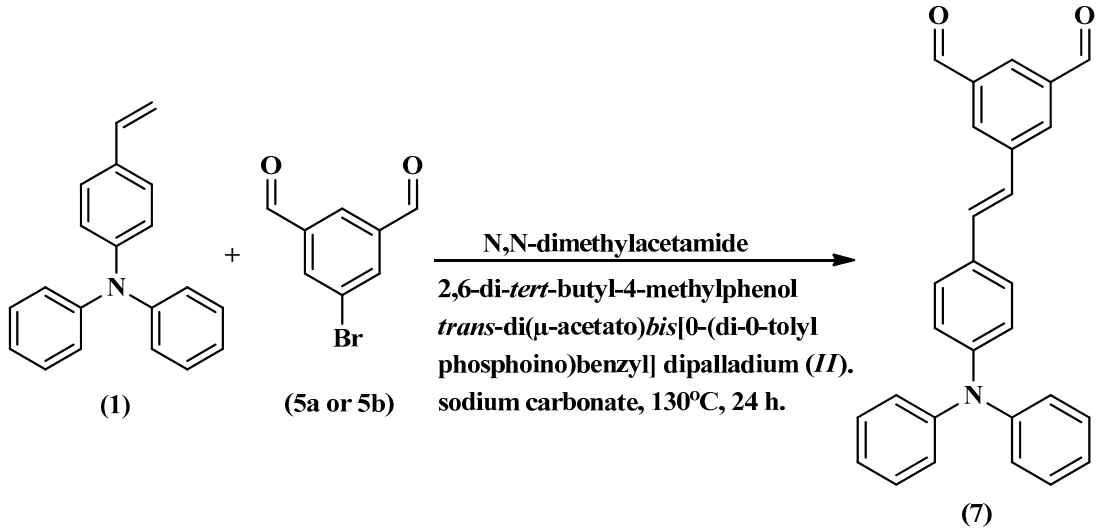

Scheme S4 Synthetic pathway of (E)-5-(4-(diphenylamino) styryl)isophthalaldehyde (7).

To a solution of diphenyl-(4-vinyl-phenyl)-amine **(1)** (1 g, 3.7 mmol) in N,N-dimethylacetamide (20 ml) was added 1,3-dimethyl 5-bromoisophthalate **(5)** (0.35 g, 0.453 mmol), 2,6-d-tert-butylmethyl phenol (0.073 gm, 0.09 mmol), anhydrous sodium carbonate (0.44 g, 1.13 mmol), and *trans*-di(μ-acetato)*bis*[0-(di-0-tolylphosphoino)benzyl] dipalladium (*II*) (0.015 g, 0.0045 mmol). The mixture was then stirred under N_2 at 130 °C for 24 h. The solution was cooled to room temperature and poured into a mixture of distilled H_2O and CH_2Cl_2 (1:1, v/v). The resulting mixture was separated by using a separation funnel. The organic layer was taken and subsequently dried over anhydrous $MgSO_4$. Rotary evaporation of the solvent under a reduced pressure was followed by high vacuum to remove the solvent. The residue was purified by column chromatography on silica gel with petroleum

spirit/diethyl ether (95:5, v/v). After that the product was tested by TLC and the product was collected after rotary evaporation of the solvent under reduced pressure to make **(7)** as a yellow solid (yield 0.4 g, 27%), m.p. 124–126 °C. A suitable crystal for X-ray structural analysis was obtained by dissolving this compound in dichloromethane followed by slow evaporation.

FTMS$^+$-MS: m/z (Accurate Mass), reference compound: NH_4OAc, calcd. for $C_{28}H_{21}NO_2$ 404.1645, found 404.1645 $[M+H]^+$. ^1H NMR (400 MHz, DMSO) δ 6.97 (d, *J* = 8.56 Hz, 2H, -*Ph*-N-Ph$_2$), 7.06 (d, *J* = 8.5 Hz, 4H, -N-*Ph*$_2$), 7.10 (t, *J* = 7.25 Hz, 2H, -N-*Ph*$_2$), 7.33 (t, *J* = 7.92 Hz, 5H, -N-*Ph*$_2$), 7.48 (d, *J* = 16.44 Hz, 1H, -*CH*=CH-Ph-), 7.58 (d, *J* = 8.85 Hz, 2H, -*Ph*-N-Ph$_2$), 8.26 (s, 1H, -*Ph*-CHO), 8.39 (s, 2H, -*Ph*-CHO), 10.13 (s, 2H, -Ph-*CHO*); ^{13}C NMR (500 MHz, DMSO-d$_6$) δ 122.52, 123.56, 124.33, 126.11, 128.28, 130.370, 130.99 (*Ar-C*-H), 125.45, 131,84, (Ar-*CH=CH*-Ar), 129.68, 134.28, 143.48 (*Ar-C*-C), 146.83, 147.45 (*Ar-C*-N), 192.70 (*C=O*). UV-Vis in ethanol: λ_{max} 296 nm, 376 nm. FT-IR spectrum (KBr) ν/cm^{-1}: 3038 cm^{-1} ν (C-H, m) aromatic; 2819, 2739 cm^{-1} ν (C-H, m) aliphatic; 1699 cm^{-1} ν (C=O, shp); 1588 cm^{-1} ν (C=C, shp) aromatic; 1492 cm^{-1} ν (C=C, shp) aliphatic; 1277 cm^{-1} ν (C-O, shp); 1176 cm^{-1} ν (C-N, m) and 963 cm^{-1} for bending (C-N).

Synthesis of 5-[(2-diphenylamino-phenyl)-vinyl]-isophthalic acid dimethyl ester (9)

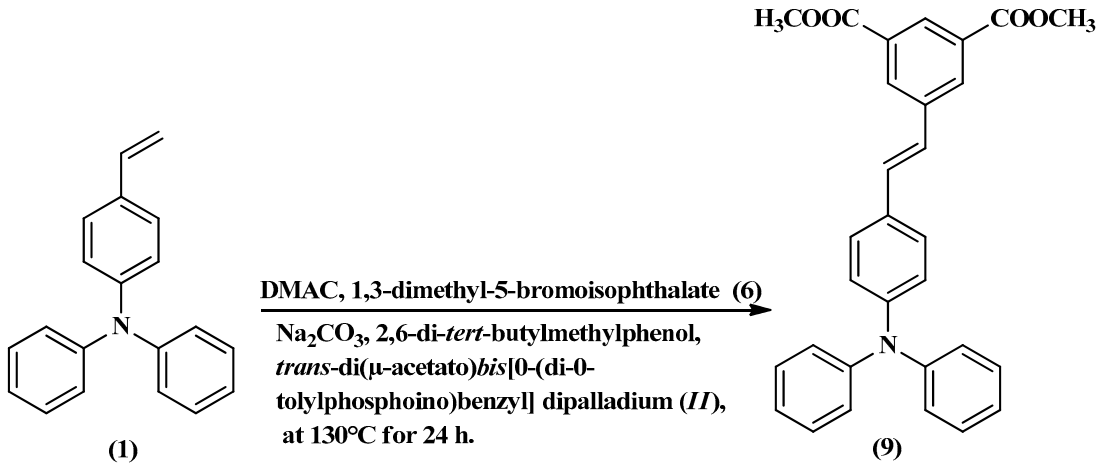

Scheme S5 Synthetic pathway of 5-[(2-diphenylamino-phenyl)-vinyl]-isophthalic acid dimethyl ester (9).

To a solution of diphenyl-(4-vinyl-phenyl)-amine **(1)** (1 g, 3.7 mmol) in N,N-dimethylacetamide (20 ml) was added 1,3-dimethyl-5-bromoisophthalate **(6)** (0.46 g, 0.453 mmol), 2,6-di-*tert*-butylmethyl phenol (0.073 g, 0.09 mmol), anhydrous Na_2CO_3 (0.44 g, 1.13 mmol), and *trans*-di(μ-acetato)*bis*[0-(di-0-tolylphosphoino)benzyl] dipalladium (*II*) (0.015 g, 0.0045 mmol). The mixture was stirred under N_2 at 130 °C for 24 h. The reaction was cooled to room temperature and poured into a mixture of distilled H_2O and CH_2Cl_2 (1:1, v/v). The mixture was separated using separation funnel, and the organic layer was taken and dried over anhydrous $MgSO_4$. After rotary evaporation of the solvent under reduced pressure and high vacuum, the residue was purified by column chromatography on silica gel with petroleum spirit/diethyl ether (95:5, v/v). After that, the product was tested using TLC and the product collected after rotary evaporation of the solvent under a reduced pressure, to give **(9)** as a yellow solid (yield 0.16 g, 11%), m.p. 110–112°C. The suitable crystal for X-ray analysis was prepared by dissolving this compound in dichloromethane followed slow evaporation.

FTMS$^+$-MS: m/z (Accurate Mass), reference compound: NH_4OAc, calcd. for $C_{30}H_{25}NO_4$ 464.1856, found 464.1852 $[M+H]^+$. ^1H NMR (DMSO-d6) δ 3.91 (s, 6H, 2x-COO*CH*$_3$), 6.96 (d, *J = 8.8*, Hz, 2H, -*Ph*-N-Ph$_2$), 7.06 (d, *J = 7.6* Hz, 4H, Ph-N-*Ph*$_2$), 7.09 (t, *J = 7.25* Hz, 2H, Ph-N-*Ph*$_2$), 7.29–7.35 (m, 5H, Ph-N-*Ph*$_2$, -*CH*=CH-Ph), 7.42 (br d, J = 16.4, 1H, -CH=*CH*-Ph), 7.60 (d, *J=8.5*Hz, 2H, -*Ph*-N-Ph$_2$), 8.33 (bs, 1H, =CH-*Ph*-COOCH$_3$), 8.38 (bs, 2H, =CH-*Ph*-COOCH$_3$); ^{13}C NMR (125 MHz, DMSO-d$_6$) δ 52.54 (-*CH*$_3$), 122.51, 123.44, 123.90, 128.06, 129.49, 130,48, 130.60 (*Ar-C*-H), 124.34, 129.60 (Ar-*CH=CH*-Ar), 133.26,

138.89, 140.17 (*Ar-C*-C), 141.74, 146.84 (*Ar-C*-N), 165.43 (*C=O*). UV-Vis in ethanol: λ_{max} 296 nm (ε = $M^{-1}cm^{-1}$), 376 nm (ε = $M^{-1}cm^{-1}$). FT-IR Spectrum (KBr) ν/cm^{-1}: 3041 cm^{-1} ν (C-H, m) aromatic; 2956, 2922 cm^{-1} ν (C-H, m) aliphatic; 1719 cm^{-1} ν (C=O, str (shp)); 1591 cm^{-1} ν (C=C, str) aromatic; 1494 cm^{-1} ν (C=C, shp) aliphatic; 1199 cm^{-1} ν (C-N, shp) and 963 cm^{-1} for ν (C-N, shp) bending.

Atomistic modelling details

Density Functional Theory

The crystal structure of anatase TiO_2 available within Materials Studio[1] was used as the parent TiO_2 surface structure, whose lattice, atomic coordinates and electronic structure were optimised using the plane wave, pseudopotential code, CASTEP[2] within the formalism of density functional theory (DFT)[3–5]. The exchange-correlation density functional was the generalised gradient approximation of Perdew, Burke and Ernzerhof (GGA-PBE)[6], and for all systems (including those containing the dye molecules) the electron-ion interactions were generated on-the-fly using the PBE functional to create consistent, norm-conserving pseudopotentials[7]. The corresponding valence electron wavefunctions were expanded by a plane wave basis set corresponding to a kinetic energy cut-off of 990 eV, giving an error bar of 5 meV between same-molecule-plus-surface systems.

For optimisation of the unit cell of TiO_2, the Brillouin zone integrations were performed on a 7 × 7 × 9 Monkhorst-Pack[8] grid with 16 symmetry constraints, and for the surface-plus-molecule and gas-phase systems the single sampling point corresponded to the gamma point. We used the pairwise, semi-empirical dispersion correction (SEDC) term of Tkatchenko and Scheffler[9] when modelling the TiO_2 surface, molecule, and surface-plus-molecule systems to account for long-range dispersions. Following the work of Martsinovich *et al.*[10] no Hubbard value was applied to Ti, which is further justified by our focus being the orientation of dye molecules on an anatase surface (rather than band gaps for example).

For all model systems (unless stated otherwise) the geometry was optimized using the method of Broyden–Fletcher–Goldfarb–Shanno (BFGS)[11] and the self-consistent electronic minimisation method was density mixing. Further convergence details per BFGS iteration are as follows: electronic energy tolerance: 10^{-8} eV; energy change per ion: dE/ion 5×10^{-6} eV; maximum force: $|F|_{max}$ 0.01 eV/Å; change in displacement: $|dR|$ 5×10^{-4} Å. All calculations were non-spin polarised. The DFT calculations were each run on 192 Intel Xeon processors - Ivy Bridge E5-2697v2 2.7GHz.

Molecular Dynamics (MD)

Vertical dye configurations with respect to the TiO_2 surface were used as the initial structure for simulations of both dyes 8 and 10. The force field parameters of the dye molecules were taken from the CHARMM General force field (CGenFF) [12–14]. During the simulation, the TiO_2 slab remained fixed. The interactions between the slab and the dye molecule are depicted by the non-bonded interaction parameters taken from the work of Brandt et al [15].

The lateral dimension of the slab is 40.84 × 30.21 $Å^2$. The anatase structure consists of 7 layers of TiO_2. 100 Å is assigned for the periodic box dimension normal to the slab surface to prevent the system from interacting with its own periodic images. After the setup, the system underwent step of minimization and 2 ns (steps) of equilibration. Simulation in NVT ensemble (constant number of particles, temperature and volume) was then performed with a time-step of 2 fs at 298 K for 40 ns. All simulations were performed using NAMD [16].

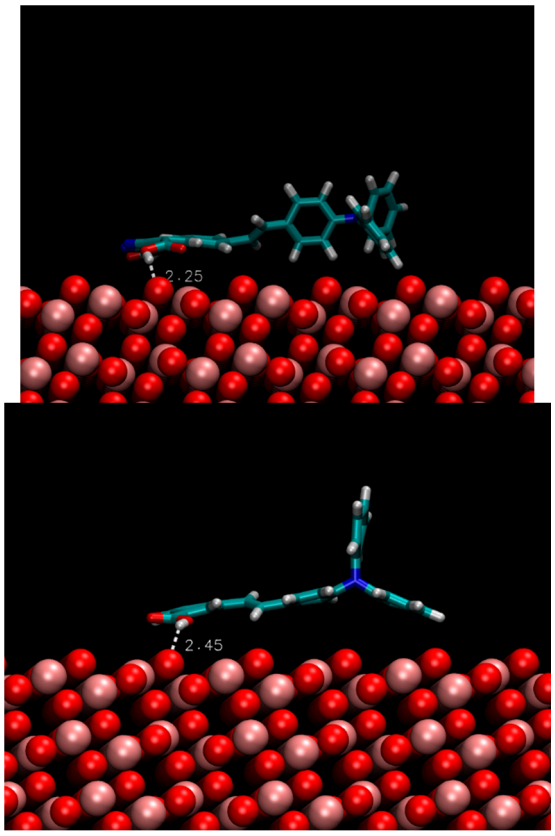

Figure 1. Snapshots from the 40 ns MD simulation of dyes (8)–LHS, and (10)–RHS. Colour scheme: O–red; Ti–pink; C–cyan; N–blue; H–white. The TiO_2 lab was kept fixed throughout the simulation.

Time Dependent Density Functional Theory (TDDFT)

Though commonly used, the TDDFT approach has several methodological limitations such as functionals, basis sets and treating double excitations. Related to the functionals a common methodological issue is inadequate description of charge transfer (CT) states by pure and hybrid functionals. This issue, however, has been addressed in recent years by using range-separated functionals [17–19]. The spectra of dyes **(8)** and **(10)** reveal occurrences of intramolecular CT hence, the range-separated functional, cam-B3LYP was used to calculate the electronic excitations. The dyes were optimized at their ground state in gas-phase using DFT and cam-B3LYP functional [20] and DFT-D3 [21] dispersion corrections. The excited states were calculated with TDDFT and the same cam-B3LYP functional. The def2-TZVP with def2/J auxiliary basis sets [22,23] - in combination with the RIJCOSX [24,25] approximation - were used for all the calculations. The spectra and the natural transition orbitals were generated via utility programs within the framework of ORCA software [26].

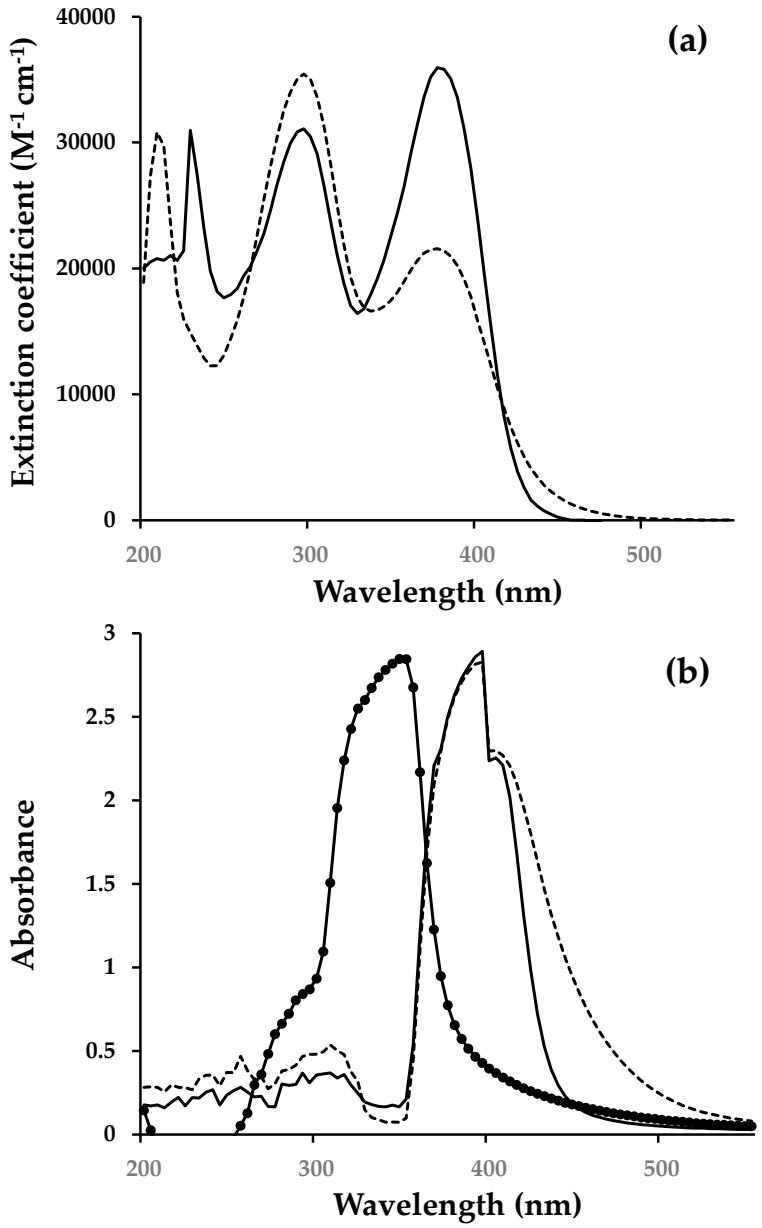

Figure S2 UV-visible spectra for (a) dyes dissolved in methanol and (b) dyes adsorbed onto a transparent, mesoporous TiO_2 film. Key: Transparent TiO_2 film–full line with circles, **(8)**–dashed line and **(10)**–full line.

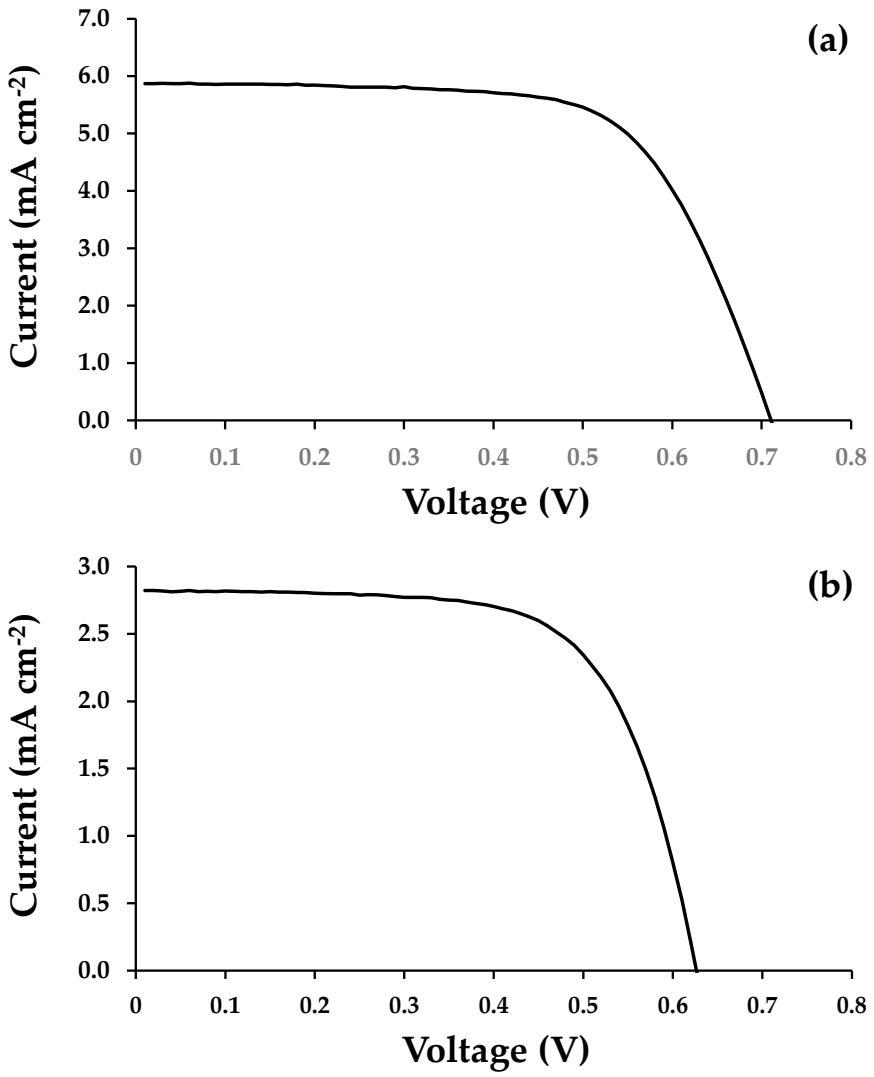

Figure 3. I-V curves for DSC devices prepared from (a) dye **(8)** and (b) dye **(10).**

Supplementary Materials References

1. Supplementary Materials References
2. Dassault Systèmes. Dassault Systèmes BIOVIA, Materials Studio v2016. San Diego: Dassault Systèmes 2016.
3. S.J. Clark, M.D. Segall, C.J. Pickard, P.J. Hasnip, M.I.J. Probert, K. Refson, M.C. Payne, *Z. Kristallogr*. 2005, 220, 567.
4. W. Kohn, L.J. Sham, *Phys. Rev.*, 1965, 140, A1133.
5. P. Hohenberg, W. Kohn, *Phys. Rev.* 1964, 136, 864.
6. M.C. Payne, M.P. Teter, D.C. Allan, T.A. Arias, J.D. Joannopoulous, *Rev. Mod. Physics.*, 1992, 64, 1045.
7. J.P. Perdew, K. Burke, M. Ernzerhof, *Phys. Rev. Letters.*, 1996, 77, 3865.
8. D.R. Hamann, M. Schlüter, C. Chiang, *Phys. Rev. Lett.*, 1979, 43(20), 1494.
9. H. Monkhorst, J. Pack, *Phys. Rev. B.*, 1976, 13, 5188.
10. A. Tkatchenko, M. Scheffler, *Phys. Rev. Lett.*, 2009, 102, 0730051.
11. N. Martsinovich, D.R. Jones, A. Troisi, *J. Phys. Chem. C.*, 2010, 114, 22659.
12. B.G. Pfrommer, M. Côté, S. Louie, M.L. Cohen, *J. Comput. Phys.* 1997, 131, 233.
13. Vanommeslaeghe, K.; Hatcher, E.; Acharya, C.; Kundu, S.; Zhong, S.; Shim, J.; Darian, E.; Guvench, O.; Lopes, P.; Vorobyov, I.; Mackerell Jr, A. D.; CHARMM general force field: A force field for drug-like molecules compatible with the CHARMM all-atom additive biological force fields. *Journal of Computational Chemistry*, **2010** *31*(4), 671–690.

14. Vanommeslaeghe, K.; MacKerell Jr, A. D.; Automation of the CHARMM General Force Field (CGenFF) I: Bond perception and atom typing. *Journal of Chemical Information and Modeling*, **2012** *52*(12), 3144–3154.
15. Vanommeslaeghe, K.; Raman, E. P.; MacKerell Jr, A. D.; Automation of the CHARMM General Force Field (CGenFF) II: Assignment of bonded parameters and partial atomic charges. *Journal of Chemical Information and Modeling*, **2012** *52*(12), 3155–3168.
16. Brandt, E. G.; Lyubartsev, A. P.; Systematic Optimization of a Force Field for Classical Simulations of TiO_2−Water Interfaces. *J. Phys. Chem. C*, **2015** 119, 18110−18125.
17. Phillips, J. C.; Braun, R.; Wang, W.; Gumbart, J.; Tajkhorshid, E.; Villa, E.; Chipot, C.; Skeel, R. D.; Kale, L.; Schulten, K. Scalable Molecular Dynamics with NAMD. J. Comput. Chem. **2005** 26, 1781−1802.
18. Fazzi, D.; Caironi, M.; Castiglioni, C. J. Am. Chem. Soc. 2011, 133, 19056−19059
19. Minami, T.; Nakano, M.; Castet, F. J. Phys. Chem. Lett. 2011, 2, 1725−1730.
20. Tamura, H.; Burghardt, I.; Tsukada, M. J. Phys. Chem. C 2011, 115, 10205−10210.
21. Yanai, T.; Tew, D. P.; Handy, N. C. Chem. Phys. Lett. 2004, 393, 51−57.
22. Grimme, S.; Antony, J.; Ehrlich, S.; Krieg, H. *J. Chem. Phys.* **2010**, *132*, 154104.
23. Weigend, F.; Ahlrichs, R. *Phys. Chem. Chem. Phys.* **2005**, *7*, 3297–3305
24. Weigend, F. Phys. Chem. Chem. Phys. 2006, 8, 1057–65.
25. F. Neese, F. Wennmohs, A. Hansen, U. Becker. *Chem. Phys.*, 2009, **356**(1), 98.
26. R. Izsák, F. Neese, *J. Chem. Phys.*, 2011, **135**(14), 144105.
27. F. Neese, WIREs: Comp. Mol. Sci., 2012, 2, 73.